

s-Process in low metallicity Pb stars

S. Bisterzo^{1,2}, R. Gallino^{2,3}, O. Straniero⁴, I. I. Ivans^{5,6}, F. Käppeler¹, and W. Aoki⁷

¹ Forschungszentrum Karlsruhe, Institut für Kernphysik, D-76021 Karlsruhe, Germany

² Dipartimento di Fisica Generale, Università di Torino, via P. Giuria 1, 10025 Torino, Italy

³ Center for Stellar and Planetary Astrophysics, School of Mathematical Sciences, PO Box 28M, Monash University, 3800 Victoria, Australia

⁴ Osservatorio Astronomico di Collurania, INAF, Teramo, 64100, Italy

⁵ The Observatories of the Carnegie Institution of Washington, Pasadena, CA, USA

⁶ Princeton University Observatory, Princeton, NJ, USA

⁷ National Astronomical Observatory, Tokyo, Japan

e-mail: bisterzo@ph.unito.it, sara.bisterzo@ik.fzk.de

Abstract. We consider a sample of very metal-poor, C-rich, s-rich and lead-rich stars observed at high-resolution spectroscopy, and some recent spectroscopic data of C+s-rich stars obtained at moderate resolution. The spectroscopic data of these stars are interpreted with AGB theoretical models of different ¹³C-pocket efficiencies, initial mass and initial r-enrichment. When lead is not measured we give our theoretical prediction. The observed stars are not on the AGB phase, but are main sequence or giant stars. They acquired the C and s enrichments by mass transfer in a close binary system from the more massive companion while on the AGB (now a white dwarf). A considerable fraction of the stars show both high s and r enrichments. To explain the s+r enriched stars we assume a parental cloud already enriched in r-elements. The measurement of Nb is an indicator of an extrinsic AGB in a binary system. The intrinsic indicator [hs/lr] constrains the initial mass, while [Pb/hs] and [Pb/lr] are a measure of the s-process efficiency. The apparent discrepancies of C and N abundances may be reconciled by assuming a strong cool bottom process occurring during the AGB. An important primary production of light elements, from Ne to Si, increasing with the star mass, is predicted for AGB models at very low metallicity, induced by n capture on primary ²²Ne and its progenies.

Key words. Stars: C and s rich – Stars: abundances – Stars: Population II – Stars: nucleosynthesis

1. Introduction

We analysed a sample of very metal-poor stars ([Fe/H] < -2) showing an enhancement in C, s elements, and lead, in several cases also in r-elements. We give an interpretation of spectroscopic abundances using AGB models of dif-

ferent s-process efficiencies, initial mass and initial r-enrichment (see Gallino et al. 2005 for further details). The estimated initial masses are in the range 1.2 to 1.5 M_{\odot} ; the ¹³C-pocket is assumed to be constant pulse by pulse. We consider a large range of ¹³C-pocket efficiencies, starting from the ST case of Gallino et al. (1998) and multiplying or dividing the ¹³C

Send offprint requests to: S. Bisterzo

abundance in the pocket by different factors. For giant stars the fit was obtained by further introducing a proper dilution factor to simulate the mixing effect of the AGB winds with the convective envelope of the observed star. To reproduce stars with both s and r enhancements, since the AGBs do not synthesise the r elements, we assumed that the parental cloud of the binary system was already enriched in r elements. The choice of the initial r-rich isotope abundance normalised to Eu is made considering the r-process solar prediction from Arlandini et al. (1999). Moreover, we selected the most significant C and s-rich stars from the sample of Barklem et al. (2005). In these cases the lead is not measured, and we give our (very high) predictions.

2. Comparison between theory and observations

All the stars considered in this paper are reported in Tables 1 and 2. In Tab. 1, fourth column, the intrinsic indicator [hs/l_s] may constrain the initial mass, while in the fifth column, [Pb/hs] is an indicator of the s-process efficiency. In the ninth column the value $[\text{Eu}/\text{Fe}]^{\text{ini}}$ corresponds to the assumed initial r-process enrichment in the progenitor cloud. The observed [Eu/Fe] is indicated by a star symbol. These values correspond to the assumed initial r-process enrichment $[\text{Eu}/\text{Fe}]^{\text{ini}}$ in the progenitor cloud. For the sample of stars by Van Eck et al. (2003), obtained at lower resolution, Eu was not measured. For these we assumed a typical $[\text{Eu}/\text{Fe}]^{\text{ini}} = 0.5$ as observed in unevolved halo stars. In Figs. 1 and 2 some examples of stars fitted with updated AGB models are shown. In Fig. 1, left panel, we report the star CS 22880-074 by Aoki et al. (2002a), with $[\text{Fe}/\text{H}] = -1.93$, fitted by an AGB model with a ¹³C-pocket of ST/10 and a dilution factor $\text{dil} = 0.30$ dex. The three lines give the uncertainties in the initial mass $M = 1.20 \pm 0.02 M_{\odot}$. No r-process enrichment is necessary; see also Bisterzo et al. (2006) for the comparison of AGB model predictions with other stars by Aoki et al. (2002a). The right panel shows the star HE 0024-2523 by Lucatello et al. (2003), with $[\text{Fe}/\text{H}] = -2.70$, fitted by an initial mass

$M = 1.3 M_{\odot}$, $\text{dil} = 0.0$ and ST/12. In Fig. 2, left panel, the giant star CS 29497-34 ($[\text{Fe}/\text{H}] = -2.90$) by Barbuy et al. (2005), is fitted with an initial mass $M = 1.5 M_{\odot}$, $\text{dil} = 1.0$, $[\text{Eu}/\text{Fe}]^{\text{ini}} = 1.5$ and ST/4. In the same plot we compare the s+r prediction (solid line) with the model without r-enrichment (dashed line) where all the heavy element abundance predictions are from the s-process. The right panel shows the fit of the recent observed star HE 0338-3945 by Jonsell et al. (2006), $[\text{Fe}/\text{H}] = -2.42$, where a best fit is obtained for an AGB model of initial $M = 1.3 M_{\odot}$ and ST/12. No dilution is necessary for this star that belongs to the main sequence. In this case a strong pre-enrichment of r elements is adopted, corresponding to $[\text{Eu}/\text{Fe}]^{\text{ini}} = 2.0$. We note that Eu is a typical r-process element and that a typical $[\text{La}/\text{Eu}]_s \approx 1$ dex is predicted. Other stars show similar r-enrichments (Tab. 1). The s-process in AGB stars produces very little Cr, Mn, and Cu. For the initial Cr and Mn we adopted the average value observed in unevolved stars in the same metallicity range (François et al. 2004). For Cu we assumed an initial solar-scaled abundance, although a subsolar value of [Cu/Fe] is in accord with unevolved stars of low metallicity (Bisterzo et al. 2004). In Fig. 3 we report the [Pb/hs] predictions as compared with observations. In the right panel stars are fitted by models of $1.3 M_{\odot}$ and in the left panel by AGB models of $1.5 M_{\odot}$. In Fig. 4, left panel, the s and r-rich star HE 0131-3953 by Barklem et al. (2005) is shown, with $[\text{Fe}/\text{H}] = -2.71$, fitted by an AGB model of $1.3 M_{\odot}$, ST/15, and $[\text{Eu}/\text{Fe}]^{\text{ini}} = 1.5$. For this star, as well as for all the other C-rich and s-rich stars in the sample of Barklem et al. (2005), lead was not measured, and we give our predictions (see Tab. 2). In particular for HE 0131-3953, we predict a value $[\text{Pb}/\text{Fe}] \approx 3.1$. The apparent discrepancies of C and N abundances may be partly reconciled by assuming a strong cool bottom process (CBP) occurring during the TP-AGB phase (Nollett et al. 2003; Wasserburg et al. 2006). Uncertainties in the spectroscopic analysis of lighter elements as C, N, O, Na, Mg and Al in very metal poor stars have been examined in detail by Asplund (2005): 3D hydrodynamical model atmospheres involve large dif-

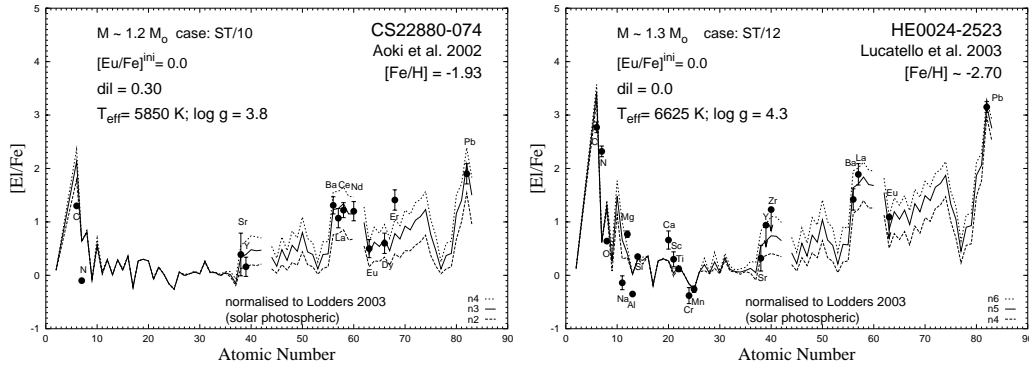


Fig. 1. Fits of two stars with updated AGB model predictions: CS 22880-074 (*Left panel*), Aoki et al. (2002a), and HE 0024-2523 (*Right panel*), Lucatello et al. (2003).

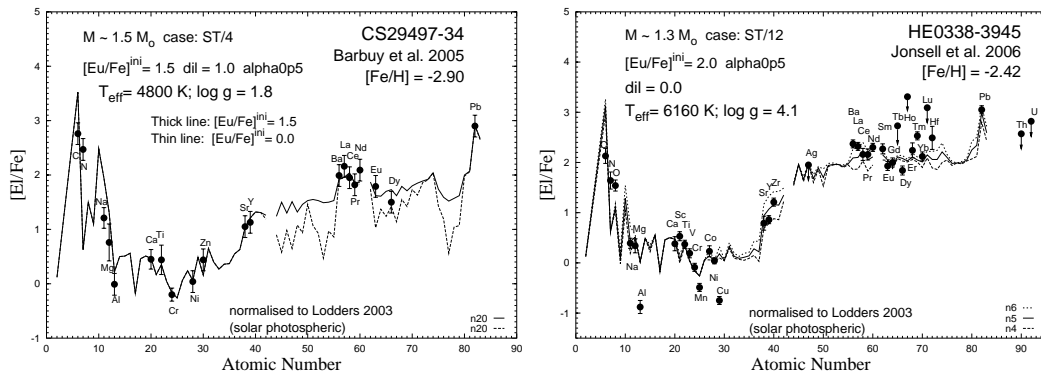


Fig. 2. *Left panel:* the CS 29497-34, Barbuy et al. (2005), fitted by s+r process (thick line) and by s-process only (thin line). *Right panel:* HE 0338-3945, Jonsell et al. (2006), with a strong r-process enhancement.

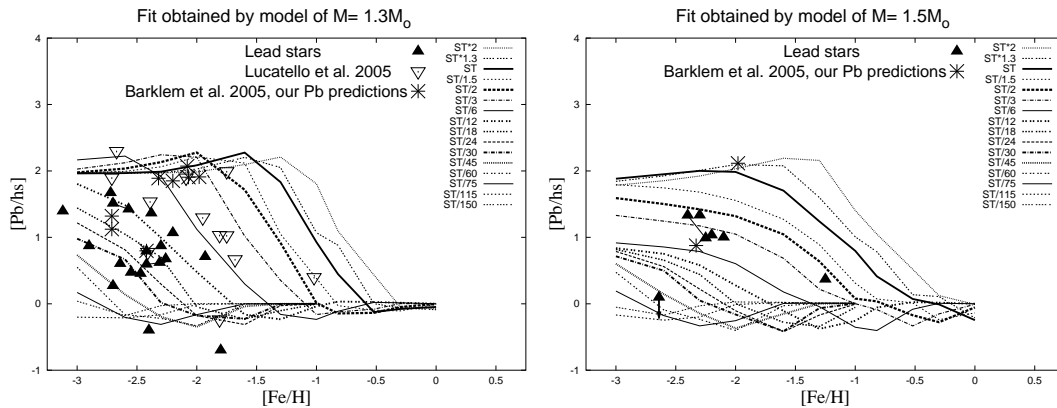


Fig. 3. $[Pb/hs]$ predictions versus metallicity for different ^{13}C -pocket compared with the spectroscopic data of s-rich and lead rich stars analysed in this paper. The two plots correspond to model of $M = 1.3 M_{\odot}$ (*Left panel*) and $M = 1.5 M_{\odot}$ (*Right panel*). With empty squares we indicate lead predictions for a selected sample of s-rich stars of Barklem et al. (2005).

Table 1. Stars sample. (*) [Eu/Fe] measured; (a) Reference code at the end of citations

Lead Stars	[Fe/H]	[Pb/Fe]	[hs/ls]	[Pb/hs]	M	Pocket	dil	[Eu/Fe] ^{int}	Ref ^a
CS 22183-015	-3.12	3.17	1.24	1.39	1.3	ST/15	0.0	1.5*	[J2]
CS 22880-074	-1.93	1.90	1.03	0.71	1.2	ST/10	0.3	0.0*	[A2a]
CS 22898-027	-2.26	2.84	1.30	0.67	1.3	ST/12	0.0	2.0*	[A2a]
CS 22942-019	-2.64	≤1.6	-0.13	≤0.09	1.5	ST/75	0.0	0.5*	[A2a]
CS 29497-030	-2.70	3.55	0.97	1.51	1.3	ST*2	0.4	0.5*	[S4]
CS 29497-030	-2.57	3.65	1.04	1.42	1.3	ST*1.3	0.0	2.0*	[I5]
CS 29526-110	-2.38	3.30	0.83	1.36	1.3	ST/6	0.0	1.5*	[A2a]
CS 30301-015	-2.64	1.70	0.81	0.60	1.3	ST/24	1.0	0.0*	[A2a]
CS 31062-012	-2.55	2.40	1.34	0.47	1.3	ST/30	0.0	1.5*	[A2a]
CS 31062-050	-2.31	2.90	1.26	0.62	1.3	ST/12	0.0	1.8*	[J4]
CS 31062-050	-2.42	2.81	1.55	0.59	1.3	ST/12	0.0	1.8*	[A2a]
LP 625-44	-2.70	2.60	1.07	0.27	1.3	ST/30	0.0	1.8*	[A2b]
HD 196944	-2.25	1.90	0.30	0.99	1.5	ST/3	1.8	0.0*	[A2a]
HD 196944	-2.40	2.10	0.17	1.33	1.5	ST/3	1.3	0.5	[V3]
HD 26	-1.25	2.00	0.73	0.37	1.5	ST/2	0.8	0.5	[V3]
HD 187861	-2.30	3.30	0.6	1.33	1.5	ST/2	0.2	0.5	[V3]
HD 189711	-1.80	0.90	0.60	-0.70	1.3	ST/24	0.4	0.5	[V3]
HD 198269	-2.20	2.40	0.93	1.07	1.2	ST/9	0.4	0.5	[V3]
HD 201626	-2.10	2.60	0.70	1.00	1.5	ST/3	0.7	0.5	[V3]
HD 224959	-2.20	3.10	1.07	1.03	1.5	ST/2	0.3	0.5	[V3]
V-Ari	-2.40	1.20	0.50	-0.40	1.2	ST/30	0.0	0.5	[V3]
HE 0024-2523	-2.70	3.30	0.56	1.67	1.3	ST/12	0.0	0.0*	[L3]
HE 2148-1247	-2.30	3.12	1.10	0.87	1.3	ST/12	0.0	2.0*	[C3]
CS 22948-27	-2.47	2.72	1.27	0.45	1.3	ST/24	0.2	1.5*	[B5]
CS 29497-34	-2.90	2.95	0.98	0.87	1.5	ST/4	1.0	1.5*	[B5]
HE 0338-3945	-2.42	3.10	1.30	0.79	1.3	ST/12	0.0	2.0*	[J6]

ferences compared with 1D models, in some cases the discrepancies are of the order of 0.5 dex. The intrinsic indicator [hs/ls] is sensitive to the initial mass. In Fig. 4, right panel, there is an example of the predicted ratio [hs/ls] versus [Fe/H], for various masses and a constant choice of the ¹³C-pocket, ST/12. A nucleosynthesis indicator of the initial mass is given by Na and Mg: at very low metallicity an important primary production, which increases with the initial mass, is predicted for these two elements in AGB models. Indeed, a strong primary production of ²²Ne results in the advanced pulses, by the conversion of primary ¹²C to ¹⁴N in the H-burning ashes, followed by double α captures on ¹⁴N in the thermal pulses, resulting in a primary production of ²³Na via ²²Ne(n, γ)²³Na, followed by a primary production of Mg from ²³Na(n, γ)²⁴Mg

and from ²²Ne(α ,n)²⁵Mg and ²²Ne(α , γ)²⁶Mg. Note that this primary production of light elements extends up to P, including Al and Si (see Fig. 5, left panel). In this figure we show the production of light elements for different masses at a given metallicity and Case ST for the ¹³C-pocket: there is a difference of up to 1.5 dex between AGB models of initial mass 1.3 and 1.5 M_{\odot} . The estimated absolute value of the initial mass depends on the choice of the mass loss rate. In the right panel our Zr and Nb predictions are shown for extrinsic (solid line) and intrinsic AGBs (dashed line). The s-process Nb is the product of the radiogenic decay of ⁹³Zr ($t_{1/2} = 1.5$ Myr), which is strongly fed by the s-process. For intrinsic AGB stars a [Zr/Nb] ≈ 1 is expected, whereas for an extrinsic AGB [Zr/Nb] ≈ 0 . Consequently [Zr/Nb] is a powerful nucleosynthesis indicator of an ex-

Table 2. Barklem et al. (2005), s-enhanced stars. (*) [Eu/Fe] measured; (^b) Pb prediction

Stars	[Fe/H]	[hs/ls]	M	Pocket	dil	[Eu/Fe]	[Pb/Fe] ^b	[Pb/hs] ^b
HE 0202-2204	-1.98	0.72	1.5	ST*1.3	0.9	0.0*	3.0	1.8
HE 0231-4016	-2.08	0.65	1.2	ST*1.3	0.0	0.0	3.4	2.1
HE 1135+0139	-2.33	0.43	1.5	ST/6	1.8	0.0*	1.8	0.9
HE 2150-0825	-1.98	0.76	1.2	ST*1.3	0.0	0.0	3.4	1.9
HE 2240-0412	-2.20	1.13	1.3	ST/6	0.0	0.0	3.2	1.8
HE 0430-4404	-2.07	0.94	1.2	ST*1.3	0.0	0.0	3.4	1.9
HE 0131-3953	-2.71	1.51	1.3	ST/15	0.0	1.5*	3.1	1.1
HE 1105+0027	-2.42	1.46	1.3	ST/12	0.0	1.8*	3.0	0.8
HE 1430-1123	-2.71	1.40	1.3	ST/15	0.0	0.0	3.1	1.3
HE 2227-4044	-2.32	0.92	1.3	ST/6	0.0	0.0	3.2	1.9

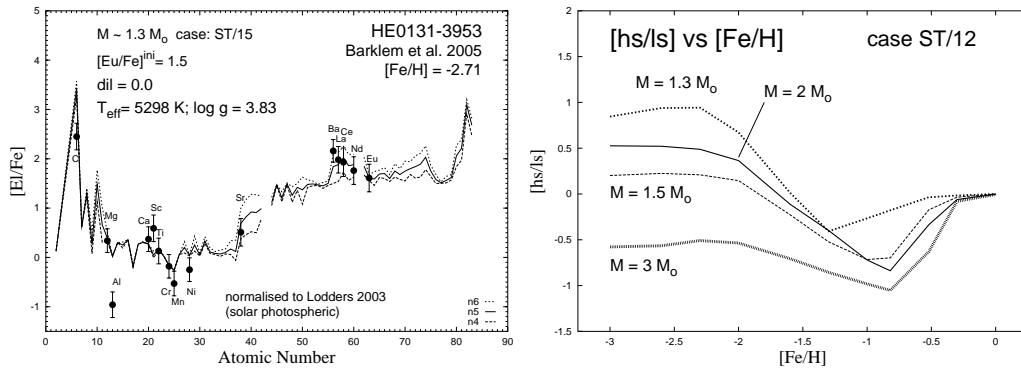


Fig. 4. Left panel: fit of HE 0131-3953, Barklem et al. (2005), where the lead is not measured. Right panel: theoretical results for [hs/ls] versus metallicity for a ¹³C-pocket of ST/12, and for different initial masses.

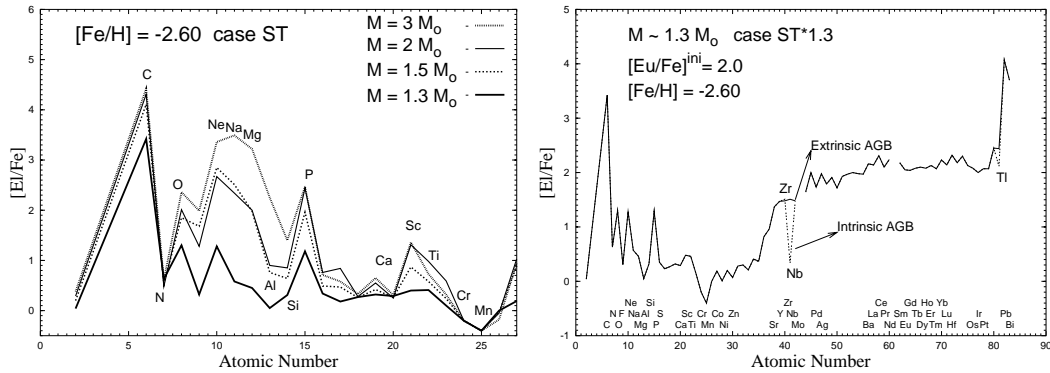


Fig. 5. Left panel: Light elements predictions for different solar masses, for the case ST at [Fe/H] = -2.6. Right panel: Zr and Nb prediction for extrinsic (solid line) and intrinsic (dashed line) AGB model of $M = 1.3 M_{\odot}$, [Fe/H] = -2.6, ST*1.3, [Eu/Fe]ⁱⁿⁱ = 2.0.

trinsic AGB in a binary system system, or of an intrinsic AGB star (Ivans et al. 2005).

3. Conclusions

We interpret C-rich, s-rich, lead-rich stars with low metallicity with AGB theoretical models of different s-process efficiencies and initial masses. The s+r enhanced stars are explained assuming that the parental cloud was triggered by a supernova pollution before the formation of the binary system. In the sample there are some C and s-rich stars without observed lead and we give our theoretical prediction. A high [Nb/Fe] value is an indicator of an extrinsic AGB in a binary system. The ratio [hs/ls] may constrain the initial mass, while [Pb/hs] and [Pb/ls] are indicators of the s-process efficiency. Other indicators of the initial mass are the Na and Mg abundances, which are produced in very low metallicity AGB stars by neutron capture on the very abundant primary ^{22}Ne . The introduction of an r-enrichment does not modify the ls, hs, and lead abundances.

Acknowledgements. MURST-FIRB project "Astrophysical Origin of the Heavy Elements beyond Iron" and the Aspen Center for Physics.

References

Asplund, M. 2005, ARA&A, 43, 481

- Aoki, W. et al. 2002a, ApJ, 580, 1149 [A02a]
 Aoki, W. et al. 2002b, Publ. Astron. Soc. Japan, 54, 427 [A02b]
 Arlandini, C. et al. 1999, ApJ, 525, 886
 Barbuy, B. et al. 2005, A&A, 429, 1031 [B5]
 Barklem, P.S. et al. 2005, A&A, 439, 129
 Bisterzo, S. et al. 2004, Mem.SAIt, 75, 741
 Bisterzo, S. et al. 2006, OMEG05 Symposium, in press
 Cohen, J.G., Christlieb, N., Qian, Y.-Z., Wasserburg, G.J. et al. 2003, ApJ, 588, 1082 [C3]
 François, P. et al. 2004, A&A, 421, 613
 Gallino, R. et al. 1998, ApJ, 497, 338
 Gallino, R. et al. 2005, IAUS, 228, 461
 Ivans, I.I., Sneden, C., Gallino, R., Cowan, J.J., Preston, G.W. et al. 2005, ApJ, 627, 145 [I5]
 Jonsell, K. et al. 2006, astro-ph/0601476 [J6]
 Johnson, J.A. & Bolte, M. 2002, ApJ, 579, L87 [J2]
 Johnson, J.A. & Bolte, M. 2004, ApJ, 605, 462 [J4]
 Lucatello, S. et al. 2003, ApJ, 125, 875 [L3]
 Lucatello, S. et al. 2005, IAUS, 228, 473
 Nollett, K.M. et al. 2003, ApJ, 582, 1036
 Sivarani, T. et al. 2004, A&A, 413, 1073 [S4]
 Van Eck, S. et al. 2003, A&A, 404, 291 [V3]
 Wasserburg, G.J. et al. 2006, astro-ph/0602551